

## Electrostatic-Field Dependent Activation Energies Modulate Electron Transfer of Cytochrome *c*

Daniel H. Murgida\* and Peter Hildebrandt

*Instituto de Tecnologia Química e Biológica, Universidade Nova de Lisboa, Apt. 127, Av. da República, P-2781-901 Oeiras, Portugal*

*Received: March 20, 2002; In Final Form: September 16, 2002*

Cytochrome *c* was electrostatically bound on Ag electrodes coated with self-assembled monolayers of carboxyl-terminated alkylthiols. Employing stationary and time-resolved surface enhanced resonance Raman spectroscopy, activation energies of the interfacial redox process were determined as a function of the electric field strength that was controlled by varying protein–electrode distance via the thiol alkyl chain length. At weak electric fields (long chain lengths), temperature- and overpotential-dependent measurements consistently yield a reorganization energy of 0.26 and 0.22 eV, respectively, which is distinctly lower than for cytochrome *c* in solution. This decrease is attributed to the lowering of the contribution of solvent reorganization for the reaction of the immobilized protein. At short alkyl chain length, high electric fields strongly raise the activation barrier for the structural reorganization of the protein and the rearrangement of the hydrogen bond network becomes rate limiting for the interfacial redox process as indicated by the H/D kinetic isotope effect that increases with the electric field strength (Murgida, D. H.; Hildebrandt, P. *J. Am. Chem. Soc.* **2001**, *123*, 4062–4068). Thus, rate constants measured as a function of the temperature provide the activation enthalpy for the underlying proton-transfer steps. The values of 24.2 and 34.3 kJ mol<sup>−1</sup> determined in H<sub>2</sub>O and D<sub>2</sub>O, respectively, as well as the ratio of the preexponential factors A(H<sub>2</sub>O)/A(D<sub>2</sub>O) of ca. 0.8 cannot be reconciled within the semiclassical description of proton transfer but indicate thermally activated nuclear tunneling. The electric-field-induced alteration of the activation barrier that controls the dynamics of the interfacial electron transfer of cytochrome *c* may represent a general mechanism for modulating biological charge-transfer dynamics at membranes.

### Introduction

In the past years, substantial progress has been achieved in elucidating long-range electron transfer (ET) reactions of redox proteins.<sup>1–3</sup> Novel experimental approaches in spectroscopy, electrochemistry, and molecular biology have opened new possibilities to determine those parameters that control ET dynamics and mechanism.

Whereas most of the previous studies refer to ET reactions of redox proteins in solution, electrochemical and spectroelectrochemical techniques have recently been established that are capable to probe ET reactions of proteins immobilized on electrodes.<sup>3–25</sup> These approaches are of particular interest not only in view of the increasing technological importance of bioelectronic devices but also for a better understanding of natural biological redox reactions that take place at membranes with permanently or temporarily bound proteins. Biological interfaces can be mimicked by electrodes coated with self-assembled monolayers (SAM) of functionalized thiols that allow electrostatic, hydrophobic, or covalent attachment of proteins. Moreover, at such functional membrane models, potential gradients are comparable to those at biomembranes such that electric fields experienced by the immobilized proteins may be similar in both cases. Previous studies have demonstrated that electric fields can influence the transfer of charges in biological

systems. In photosynthetic reaction centers, the rate of charge recombination is altered by up to 1 order of magnitude upon applying external electric fields of ca. 10<sup>6</sup> V/cm.<sup>26–28</sup> However, the methods employed in these studies do not provide any information on *how* electric fields may affect ET reactions because driving force, electronic coupling parameter, reorganization energy, as well as molecular structures cannot be explicitly controlled or determined.

Employing surface enhanced resonance Raman (SERR) spectroscopy, we have recently introduced a new approach for studying ET reactions of Cyt-*c* immobilized on SAM-coated Ag electrodes.<sup>17–20,24</sup> This technique selectively probes the vibrational spectrum of the heme solely of the adsorbed proteins and is capable to distinguish between those species that differ with respect to their redox site structure. Potential-dependent stationary and time-resolved (TR) SERR spectroscopy thus allows us to analyze the thermodynamics and kinetics of the interfacial processes including ET and non-Faradaic reactions. Using SAMs of different chain lengths, it is possible to vary systematically the separation of the bound Cyt-*c* from the electrode and, hence, the potential drop across the interface that controls the electric field acting on the protein.<sup>18</sup> In these studies, we have shown that the interfacial ET kinetics of Cyt-*c* at long chains (weak electric fields) displays a normal exponential distance dependence. At chain lengths shorter than 12 Å, the rate constant approaches a limiting value of ca. 130 s<sup>−1</sup>.<sup>19</sup> The onset of the nonexponential behavior is accompanied by an H/D

\* To whom correspondence should be addressed. Phone: +351-21-446-9717. Fax: +351-21-441-1277. E-mail: murgida@itqb.unl.pt.

kinetic isotope effect (KIE) that increases up to 4 at ca. 7 Å. Thus, it was suggested that proton transfer (PT), associated with the redox-linked rearrangement of the hydrogen bonding network in the protein, becomes rate-limiting because of an electric-field-induced increase of the underlying activation barrier(s) at short chain lengths.

The present work is dedicated to checking this hypothesis and to elucidating the mechanism of the interfacial redox process of Cyt-*c* in more detail. By means of TR SERR spectroscopy, we have determined the ET rate constants as a function of the overpotential ( $\eta$ ) and the temperature at long and short chain lengths to analyze the electric field effects on the activation energies of the individual reaction steps involved.

## Materials and Methods

**Methods.** SERR spectra were measured with the 413 nm excitation line of a Kr<sup>+</sup> laser (Coherent Innova 302) using a spectrograph (U1000, ISA) equipped with a liquid-nitrogen-cooled CCD camera. The spectral resolution was 4 cm<sup>-1</sup>, and the step width (increment per data point) was 0.53 cm<sup>-1</sup>. The laser beam (ca. 60 mW) was focused onto the surface of a rotating Ag electrode in a home-built thermostated (nonisothermal) electrochemical cell, which permits temperature control within  $\pm 0.1$  °C. The SAM-modified Ag electrode was in contact with a solution containing the supporting electrolyte (12.5 mM potassium phosphate buffer at pH = 7 and 12.5 mM K<sub>2</sub>SO<sub>4</sub>) and 0.1  $\mu$ M Cyt-*c*. All potentials cited in this work refer to the saturated calomel electrode (SCE).

In TR SERR experiments, a rapid potential jump was applied, and the relaxation process was probed by SERR spectroscopy after a delay time  $\delta$  during a measuring interval  $\Delta t$ . The sequence of potential jumps, delay times, and measuring intervals was controlled by a home-built electronic timer that is linked to the potentiostat and an optoelectronic intensity modulator for gating the laser excitation. The time-resolution was exclusively limited by the response time of the electrochemical cell, which was estimated to be faster than 150  $\mu$ s. Further details of the experimental setups and the methodology are given elsewhere.<sup>18,19,29</sup> Stationary and TR SERR spectra were analyzed quantitatively by fitting the component spectra of the individual species to the measured spectra.<sup>30</sup>

Maximum errors for the reorganization energies determined from overpotential- and temperature-dependent measurements are estimated to be 10% and 20%, respectively. The errors for the activation enthalpies and entropies are ca. 10%.

**Materials.** Following electrochemical roughening, the Ag electrode was immersed in a 2 mM ethanolic solution of  $\omega$ -carboxyl alkanethiols for 24 h and subsequently rinsed with ethanol and dried. Further details of the treatment and coating of the electrodes are given elsewhere.<sup>18</sup> Cyt-*c* from horse heart (Sigma, type VI) was purified according to standard procedures.<sup>31</sup> All chemicals were of highest purity grade available.

## Results and Discussion

**Activation Barrier at Low Electric Field.** SAMs of 16-mercaptohexadecanoic acid (C<sub>16</sub>) represent a good compromise between a large distance to the electrode (low field) and a still acceptable SERR intensity.<sup>18</sup> TR SERR spectra of adsorbed Cyt-*c* were measured at various  $\delta$  after applying a negative potential jump to different final potentials corresponding to different driving forces for the ET. In these experiments, the temperature was kept constant at 20 °C. All spectra could be quantitatively simulated on the basis of the component spectra of solely the reduced and oxidized native Cyt-*c*.<sup>19</sup> Thus, there

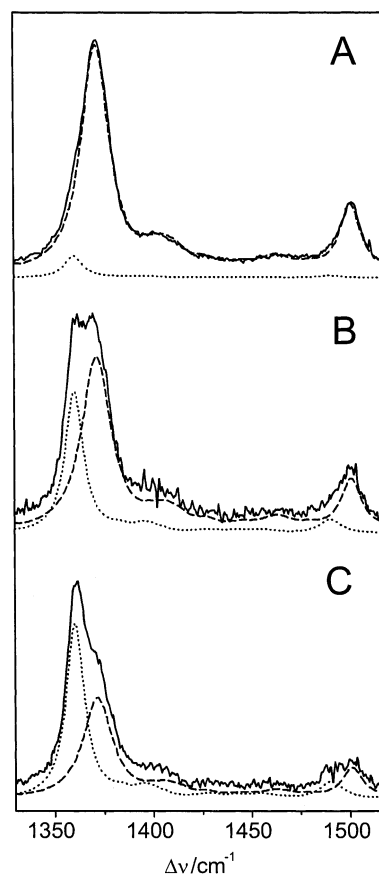


**Figure 1.** TR SERR spectra of Cyt-*c* immobilized on C<sub>16</sub>-SAM coated Ag electrodes, measured with 413 nm excitation and  $\delta = 180$  ms after a potential jump from +0.106 V to different final potentials that correspond to overpotentials of (A) 0.0, (B) -0.2, and (C) -0.4 V. All potentials refer to SCE. The dotted and the dashed lines represent the component spectra of the reduced and oxidized Cyt-*c*, respectively.

is no indication for the involvement of intermediate states in the heterogeneous ET that, hence, was analyzed in terms of a one-step relaxation process. In fact, the relaxation kinetics was found to be monophasic except for very high values of  $\eta$  where slow potential-dependent reorientation of the immobilized protein leads to a second phase.<sup>17</sup> The selection of spectra in Figure 1, measured at  $\delta = 180$  ms, illustrate the effect of increasing  $\eta$  on the progress of Cyt-*c* reduction. Logarithmic plots of the relative concentrations derived from the TR SERR spectra as a function of  $\delta$  (data not shown) yielded ET rate constants for different  $\eta$  [ $k_{ET}(\eta)$ ], which were analyzed according to electrochemical ET theory (eq 1):<sup>2,5,32</sup>

$$k_{ET}(\eta) = k_{ET}(0) \frac{1 - \operatorname{erf} \frac{F\eta + \lambda}{2\sqrt{\lambda RT}}}{1 - \operatorname{erf} \frac{\lambda}{2\sqrt{\lambda RT}}} \quad (1)$$

where  $k_{ET}(0)$  is the formal heterogeneous ET rate constant ( $\eta = 0$  V) and  $F$ ,  $R$ , and  $T$  have the usual meaning. Equation 1 provides an excellent fit to these data with a reorganization energy ( $\lambda$ ) of 21.2 kJ mol<sup>-1</sup> corresponding to 0.22 electronvolt (eV; Figure 2).

Temperature-dependent measurements represent an alternative approach for determining  $\lambda$ . In the temperature range between 5 and 25 °C, the redox equilibria determined from potential-dependent stationary SERR experiments follow an ideal Nernstian behavior. The redox potentials ( $E^0$ ) obtained in this way

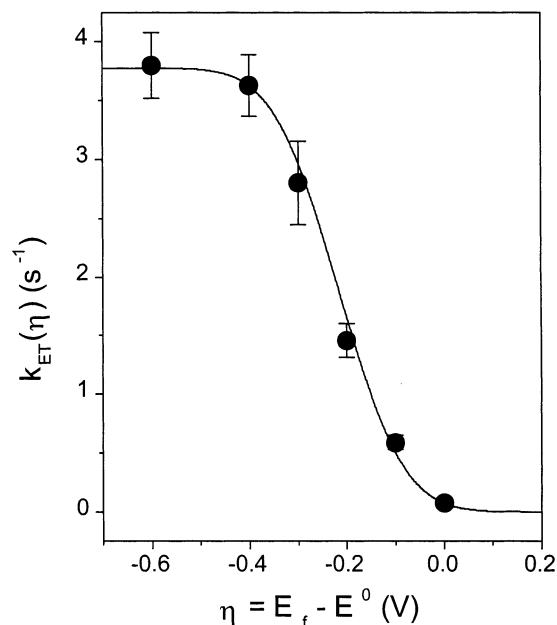


**Figure 2.** Plot of  $k_{\text{ET}}$  as a function of  $\eta$  (solid circles). The solid line represents the best fit ( $\lambda = 0.22 \text{ eV mol}^{-1}$ ) of eq 1 to the experimental data that were obtained from TR SERR spectra for Cyt-*c* immobilized on C<sub>16</sub> SAM coated Ag electrodes.

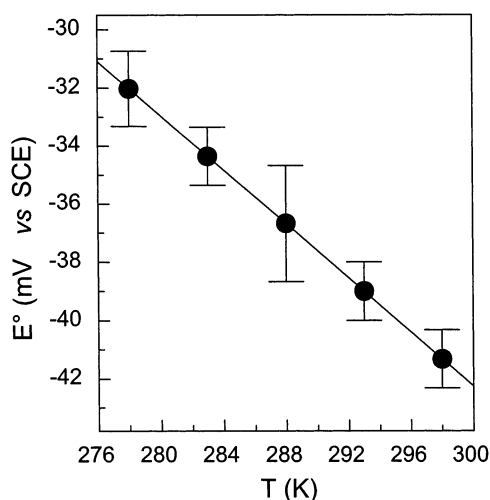


**Figure 3.** Temperature-dependence of the redox potentials (vs SCE) determined from stationary SERR spectra for Cyt-*c* immobilized on C<sub>16</sub>-SAM coated Ag electrodes.

display the expected linear temperature dependence (Figure 3), which allows us to determine the reaction entropy  $\Delta S^0$  according to

$$\Delta S^0 = S_{\text{ox}}^0 - S_{\text{red}}^0 = -F \left( \frac{dE^0}{dT} \right) \quad (2)$$

The reaction entropy of  $45 \text{ J K}^{-1} \text{ mol}^{-1}$  that is obtained from these data is only slightly lower than the values reported previously for nonimmobilized Cyt-*c* (ca.  $55 \text{ J K}^{-1} \text{ mol}^{-1}$ ).<sup>33</sup>

Subsequently, TR SERR measurements were carried out in the temperature range from 5 to 20 °C by applying positive potential jumps to  $E^0(T)$  to determine  $k_{\text{ET}}(0)$ . The temperature-dependence of  $k_{\text{ET}}(0)$  can be approximated by

$$k_{\text{ET}}(0) = \frac{C}{\sqrt{T}} \exp \left( -\frac{\Delta H^\ddagger}{RT} \right) \quad (3)$$

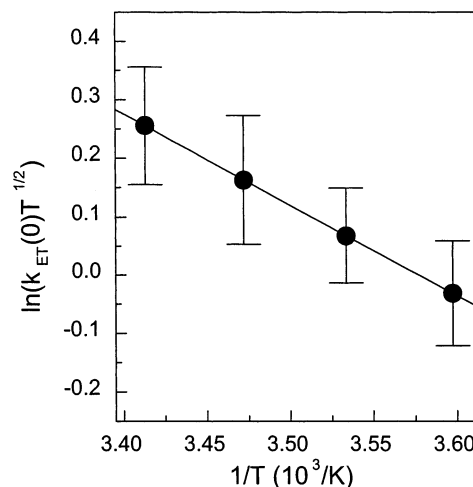


**Figure 4.** Semilogarithmic plot of  $k_{\text{ET}}(0)T^{1/2}$  for Cyt-*c* immobilized on C<sub>16</sub>-SAM coated Ag electrodes versus  $1/T$  according to eq 3. The experimental data were obtained from TR SERR experiments with potential jumps to the redox potential.

assuming that the electronic coupling parameter and  $\lambda$ , which are included in the constant  $C$ , are independent of temperature within this range.<sup>34</sup> A plot of  $\ln(k_{\text{ET}}(0)T^{1/2})$  vs  $1/T$  yields a straight line (Figure 4) from which  $\Delta H^\ddagger$  is calculated to be  $13 \text{ kJ mol}^{-1}$ . Using eq 4

$$\Delta S^\ddagger = \frac{1}{2} \Delta S^0 \quad (4)$$

one obtains  $\Delta G^\ddagger = 6.3 \text{ kJ mol}^{-1}$ , which according to eq 5<sup>34</sup>

$$\lambda = 4\Delta G^\ddagger \quad (5)$$

yields a reorganization energy of  $25.1 \text{ kJ mol}^{-1}$  corresponding to  $0.26 \text{ eV}$ . Within the temperature range used in this study (5–25 °C), no species other than the reduced and oxidized native Cyt-*c* were detectable in the stationary or TR SERR spectra implying that temperature-dependent and  $\eta$ -dependent measurements probe the same process. In fact, the values for  $\lambda$  determined by both approaches agree very well within the experimental accuracy, which is considered to be somewhat lower for the  $T$ -dependent than for the  $\eta$ -dependent experiments.<sup>35</sup> This agreement also implies that reorganization energies for reduction and oxidation are the same since  $\eta$ - and  $T$ -dependent experiments were carried out with potential jumps of opposite sign. Furthermore, both methods afford the same activation parameters ( $\Delta S^\ddagger$ ,  $\Delta H^\ddagger$ , and  $\lambda$ ) in H<sub>2</sub>O and D<sub>2</sub>O, which is in line with our previous observations that the formal heterogeneous ET constant does not exhibit a kinetic H/D isotope effect when Cyt-*c* is immobilized on SAMs of C<sub>16</sub> or 11-mercaptopundecanoic acid (C<sub>11</sub>).<sup>19</sup> Hence, it is concluded that  $\lambda$  derived from the  $T$  and  $\eta$  dependence of  $k_{\text{ET}}$  exclusively refer to the ET process of the immobilized Cyt-*c* in its native structure.

In previous studies, the reorganization energy of Cyt-*c* has been determined from photoinduced ET processes or by cyclic voltammetry yielding values in the range from 0.58 to 1.5 eV,<sup>1a,36,37</sup> among which the most reliable value is probably ca. 0.6 eV. However, all of these studies refer to the ET of Cyt-*c* in solution such that the substantially lower value determined in this work evidently reflects an intrinsic property of the ET process of the immobilized protein. Note that a relatively low reorganization energy (0.28–0.35 eV) of adsorbed Cyt-*c* was already derived from previous cyclic voltammetry experiments

although the result was considered to be associated with a substantial uncertainty.<sup>4,5</sup> Also for myoglobin immobilized on a pyrolytic graphite electrode, the reorganization was drastically lowered compared to the protein in solution.<sup>16</sup>

The total reorganization energy  $\lambda$  includes contributions of the heme pocket ( $\lambda_{RC}$ ), the surrounding protein ( $\lambda_P$ ), and the solvent ( $\lambda_S$ ).<sup>34</sup> SERR spectra of oxidized and reduced Cyt-*c* are identical to the corresponding resonance Raman spectra measured for the protein in solution such that adsorption-induced structural changes of the heme pocket and thus alterations of  $\lambda_{RC}$  can largely be ruled out.<sup>17–19</sup> Conversely, subtle protein structural changes that are not visible in the SERR spectra are likely to occur in the binding domain. Such changes may indeed alter  $\lambda_P$  because this protein region includes the peptide segment 78–87, which in solution displays notable redox-linked changes of the hydrogen bond network.<sup>38</sup> Whereas this effect on  $\lambda_P$  is difficult to assess,  $\lambda_S$  should be distinctly lowered because of the partial exclusion of water molecules from the binding domain, which in solution are expected to provide the major contribution to  $\lambda_S$  in view of their proximity to the redox site. Also for the remaining solvent molecules in the hydration shell of the immobilized protein, the reorganization energy should be reduced because of the lowering of the static dielectric constant in the electrical double layer of the SAM/solvent interface.<sup>16,34</sup> Hence, a substantial decrease of  $\lambda_S$ , which along with  $\lambda_P$  is predicted to provide 60–90% of the total reorganization energy,<sup>39,40</sup> may well account for the lowering of the total reorganization energy from  $\sim 0.6$  to  $\sim 0.22$  eV. In contrast to the alterations of the Franck–Condon term, the electronic coupling term of the ET does not appear to be affected upon binding to C<sub>16</sub>- and C<sub>11</sub>-SAMs inasmuch as its distance-dependence displays a normal behavior similar to that determined for ET reactions of Cyt-*c* in solution.<sup>19</sup>

**Activation Barrier at High Electric Field.** Upon binding of Cyt-*c* to SAMs of chain length shorter than C<sub>11</sub>, that is under strong electric fields, PT becomes the rate-limiting step of the redox process as indicated by the nonexponential distance dependence and the increasing KIE. In this regime (e.g., C<sub>3</sub>-SAMs; Figure 5),  $\eta$ -dependent TR SERR do not allow for the determination of the reorganization energy. In fact, raising the overpotential causes only a slight increase of the reduction rate constant, which would formally correspond to a reorganization energy of ca. 0.02 eV as compared to 0.22 eV at long SAM lengths. Conversely,  $T$ -dependent measurements yield substantially higher activation barriers for the redox process of Cyt-*c* on C<sub>3</sub>-SAM. According to eq 6

$$\ln\left(\frac{k_{ET}(0)}{T}\right) = \ln A - \frac{\Delta H^\ddagger}{RT} \quad (6)$$

$\Delta H^\ddagger$  was determined to be 24.2 and 34.3 kJ mol<sup>−1</sup> in H<sub>2</sub>O and in D<sub>2</sub>O, respectively, and the ratio of the preexponential factors  $A(D_2O)/A(H_2O)$  is 0.82 (Figure 6). Note that temperature-dependent stationary measurements in both H<sub>2</sub>O and D<sub>2</sub>O afforded approximately the same value for  $\Delta S^\circ$  as at long chain lengths. Taking into account a correction for the interfacial potential drop,<sup>41</sup> also the redox potential is invariant implying that the thermodynamic parameters  $\Delta H^\circ$  and  $\Delta S^\circ$  of the *entire* redox process are largely independent of the electric field and the solvent.

The kinetic experiments in the high electric field region refer to the rate-limiting PT that is likely to be associated with the changes in the hydrogen bond network in the protein as required for the transition between the reduced and the oxidized Cyt-*c*.<sup>38,42</sup> Whereas at weak electric fields this structural reorganiza-

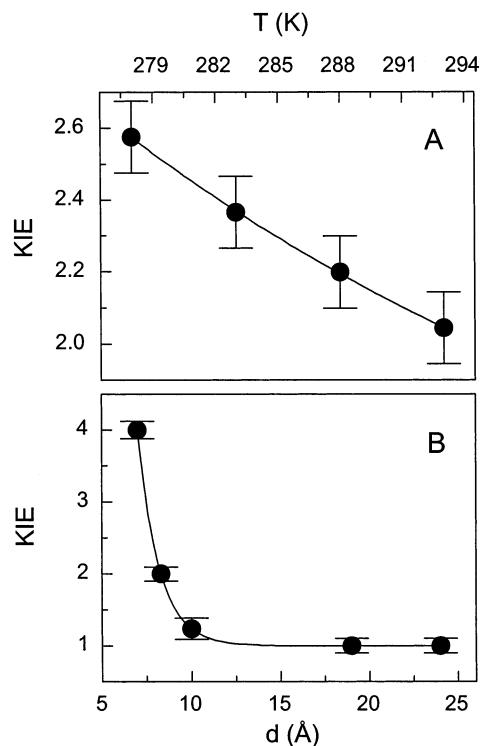


**Figure 5.** Dependence of KIE on (A) the temperature and (B) the SAM length  $d$ . Data for B were taken from ref 19.

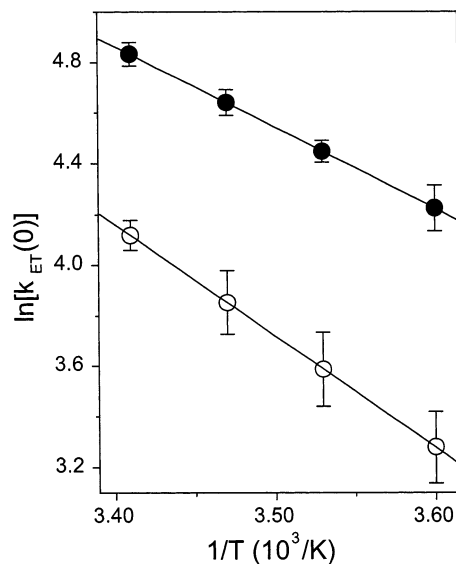


**Figure 6.** Eyring plots of  $k_{ET}(0)$  measured as a function of the temperature for Cyt-*c* immobilized on C<sub>3</sub>-SAM coated Ag electrodes in H<sub>2</sub>O (solid circles) and D<sub>2</sub>O solutions (open circles). The experimental data were obtained from TR SERR experiments with potential jumps to the redox potential.

tion takes place with  $(\lambda_{RC} + \lambda_P) < 0.22$  eV, strong electric fields drastically raise the activation barrier for (one or more) of the underlying PT steps. Such an electric-field induced barrier increase may result from the induction and alignment of dipole moments and shifts of acid–base equilibria in the protein.<sup>43,44</sup>

Within the framework of semiclassical over-the-barrier H/D transfer, the activation enthalpy difference  $[\Delta H^\ddagger(D_2O) - \Delta H^\ddagger(H_2O)]$  of 10.1 kJ/mol and the ratio  $A(D_2O)/A(H_2O)$  of 0.82 cannot account for the KIE of 2.0 at C<sub>3</sub>-SAM (20 °C). Conversely, this KIE value would correspond to an activation enthalpy difference of ca. 2 kJ/mol, which is lower by a factor



of 5 than the experimental result. Therefore, a quantum mechanical under-the-barrier tunneling has to be considered.

As the underlying PT occurs in a hydrogen-bonded system, donor–acceptor interactions are relatively strong such that nuclear tunneling must occur in the partially adiabatic (or even fully adiabatic) regime.<sup>2,45,46</sup> In this case and for a fixed donor–acceptor distance, Arrhenius plots are expected to yield similar activation enthalpies in H<sub>2</sub>O and D<sub>2</sub>O but a large A(H<sub>2</sub>O)/A(D<sub>2</sub>O) ratio because tunneling probability, included in the preexponential factor, is higher for the lighter nucleus. Typical examples that display such a kinetic behavior have been reported for various enzymatic reactions involving C–H bond cleavage.<sup>46–50</sup> The situation is different for systems in which the donor–acceptor distance can vary because of subtle structural fluctuations of the environment.<sup>46</sup> Then, the optimum tunneling distances corresponding to high tunneling probabilities can be achieved for both nuclei but at the expense of higher energy expenditure for the heavier nucleus. As a consequence, the A(H<sub>2</sub>O)/A(D<sub>2</sub>O) ratio may approach unity, whereas the activation enthalpy becomes larger for deuteron compared to proton tunneling such that the KIE decreases with increasing temperature as it was for instance observed for enzymatic reactions of alcohol dehydrogenase and methylamine dehydrogenase.<sup>48,50,51</sup> This tunneling mechanism can consistently explain the kinetic data for Cyt-*c* immobilized on SAMs of short chain lengths determined in this work. An alternative interpretation that as well can account for the present results assumes the interplay between semiclassical and quantum mechanical proton/deuteron transfer.<sup>48,49</sup> On the basis of this model, a tunneling contribution at least for proton transfer in Cyt-*c* is required to describe the experimental findings. This mechanism is operative when strong electric fields raise the activation energy barrier(s) of critical step(s) in protein reorganization. It may well be that in the absence of electric fields the barriers are sufficiently low and broad to favor fast classical PT such that electron tunneling is rate-limiting even at short transfer distances.

The results of the present study rule out alternative explanations that are (largely) based on structural differences in H<sub>2</sub>O and D<sub>2</sub>O as proposed previously.<sup>52–54</sup> For example, azurin exhibits different reduction potentials, reaction and activation entropies, which were interpreted in terms of slightly different driving forces and thermal expansions of the protein in both solvents.<sup>52</sup> Such an interpretation cannot account for Cyt-*c* immobilized on electrodes because in H<sub>2</sub>O and D<sub>2</sub>O redox potentials and reaction entropies are the same within the experimental accuracy ( $\pm 2$  mV;  $\pm 5$  J K<sup>−1</sup> mol<sup>−1</sup>), and SERR spectra were found to be identical ruling out structural differences at the redox site. Both the reaction entropies and the SERR spectra remain unchanged in the temperature range under consideration<sup>55</sup> and do not vary with the SAM chain length,<sup>41</sup> in contrast to the KIE that strongly increases with the electric field strength and decreases upon raising the temperature (Figure 5).

The electric-field induced energetic and kinetic separation of protein structural reorganization and electron tunneling<sup>56</sup> can readily account for previous findings for Cyt-*c* electrostatically immobilized on Au electrodes.<sup>15,25</sup> Upon hydrophobic immobilisation, however, electric field effects may remain relatively weak because for Cyt-*c* bound to alkyl-terminated SAMs no retardation of proton-coupled ET was observed even for very short distances.<sup>57</sup> Thus, the strikingly low values for the apparent reorganization energy of hydrophobically bound azurin<sup>21,23</sup> and the deviation from the exponential distance dependence of the ET rate constant<sup>21</sup> may reflect a conformationally gated rather than an electric-field controlled interfacial redox process.

**Electric Field Control of Interfacial Charge-Transfer Reactions.** A nonexponential distance-dependence of the interfacial ET reaction has also been observed for electrostatically immobilized tetraheme protein cytochrome *c*<sub>3</sub>,<sup>58</sup> indicating that the electric field induced perturbation of the protein structural reorganization is not an unique phenomenon of Cyt-*c*. Furthermore, these electric field effects are not necessarily linked to a redox process but are also relevant for conformational transitions. The reversible transition of ferric Cyt-*c* from its native state to the conformational state B2 that is associated with a ligand exchange takes place on the long millisecond time scale upon electrostatic binding to bare electrodes (high electric fields), but this ligand exchange process (Met-80 → His-33) is substantially accelerated upon hydrophobic immobilization.<sup>29,57,59</sup> Also, this reaction requires a rearrangement of the hydrogen bonding network in the protein and hence may be affected by the electric-field-induced alteration of the activation energy for the PT steps. The same explanation may hold for the potential-dependence of the photocycle kinetics of sensory rhodopsin II inasmuch as the underlying structural changes include de- and re-protonation of the retinal Schiff base (unpublished results).

Because many biological processes are associated with changes of hydrogen bonding interactions, electric field effects can be expected for a variety of proteins and enzymes and not only in reactions at electrodes but also at any types of charged interfaces of sufficiently high electric fields including biological membranes. We therefore propose that the electric-field dependence of the reorganization energy constitutes a general mechanism for modulating the dynamics of biological charge transfer. Specifically, the present results may contribute to a better understanding of the redox reaction of Cyt-*c* with the membrane-bound cytochrome *c* oxidase (CcO).<sup>60</sup> Formation of the electrostatically stabilized Cyt-*c*/CcO complex should lower the reorganization energy of Cyt-*c* to a value similar to that determined at C<sub>16</sub>-SAMs. This may be essential for the fast interprotein ET in the absence of external electric fields that proceeds with ca. 10<sup>5</sup> s<sup>−1</sup>.<sup>61,62</sup> even though the driving force is ca. 0 eV.<sup>63</sup> The generation of a proton gradient during enzymatic turnover and concomitant increase of the electric field may then raise the energy barriers for the interprotein ET and the intramolecular charge-transfer processes in CcO, which thus can constitute a feedback inhibition mechanism to avoid unproductive oxygen reduction by CcO.

Following this idea, an electric-field-induced increase of the potential energy barrier for proton tunneling may also exert a regulatory function for molecular proton pumps that are not linked to ET. As a possible example, we refer to the potential-dependence of the photocycle kinetics of bacteriorhodopsin, which in turn controls the proton pump activity.<sup>64</sup>

The electric-field dependence of the reorganization process in ET reactions described in this work is also of potential importance for a variety of technological applications that are based on electrode reactions such as electrocatalysis or bioelectronics. Proper choice of the electrode material and coatings may allow varying electric fields such that critical reaction steps are either slowed or accelerated, depending on the demands of the specific device.

## Conclusions

1. For electrostatically immobilized Cyt-*c* at low electric fields (long SAM lengths), the reorganization energy of the ET is substantially smaller compared to the reaction of the protein in solution. This lowering is attributed to distinctly lower contribution of the solvent reorganization energy.

2. Upon increasing the electric field strength (decreasing SAM length), the activation barrier for the redox linked rearrangement of the hydrogen bond network in Cyt-*c* strongly increases such that PT becomes rate-limiting for the interfacial ET.

3. This proton translocation, at least partially, does not proceed via a classical over-the-barrier movement. A mechanism in which tunneling is supported by thermally activated structural fluctuations of the protein provides a consistent explanation for the experimental data.

4. Electric-field-induced modulation of activation energies may constitute a general mechanism for controlling charge transfer across biological interfaces.

**Acknowledgment.** P.H. acknowledges support from the Volkswagen-Stiftung.

## References and Notes

- (1) (a) Gray, H. B.; Winkler, J. R. *Annu. Rev. Biochem.* **1996**, *256*, 537–561. (b) Page, C. G.; Moser, C. C.; Chen, X.; Dutton, P. L. *Nature* **1999**, *402*, 47–52.
- (2) Kuznetsov, A. M.; Ulstrup, J. *Electron transfer in chemistry and biology. An introduction to the theory*; Wiley: New York, 1999.
- (3) Armstrong, F. A.; Wilson, G. S. *Electrochim. Acta* **2000**, *45*, 2623–2645.
- (4) Song, S.; Clark, R. A.; Bowden, E. F.; Tarlov, M. J. *J. Phys. Chem.* **1993**, *97*, 6564–6572.
- (5) Nahir, T. M.; Clark, R. A.; Bowden, E. F. *Anal. Chem.* **1994**, *66*, 2595–2598.
- (6) Armstrong, F. A.; Heering, H. A.; Hirst, J. *Chem. Soc. Rev.* **1997**, *26*, 169–179.
- (7) Feng, Z. Q.; Imabayashi, S.; Kakiuchi, T.; Niki, K. *J. Chem. Soc., Faraday Trans.* **1997**, *93*, 1367–1370.
- (8) Ruzgas, T.; Wong, L.; Gaigalas, A. K.; Vilker, V. L. *Langmuir* **1998**, *14*, 7298–7305.
- (9) Rusling, J. F. *Acc. Chem. Res.* **1998**, *31*, 363–369.
- (10) Bayachou, M.; Lin, R.; Cho, W.; Farmer, P. J. *J. Am. Chem. Soc.* **1998**, *120*, 9888–9893.
- (11) El Kasmi, A.; Wallace, J. M.; Bowden, E. F.; Binet, S. M.; Linderman, R. J. *J. Am. Chem. Soc.* **1998**, *120*, 225–226.
- (12) Friis, E. P.; Anderson, J. E. T.; Kharkats, Yu. I.; Kuznetsov, A.; Nichols, R. J.; Zhang, J. D.; Ulstrup, J. *Proc. Natl. Acad. Sci. U.S.A.* **1999**, *96*, 1379–1384.
- (13) Gaigalas, A. K.; Ruzgas, T. *J. Electroanal. Chem.* **1999**, *465*, 96–101.
- (14) Fedurco, M. *Coord. Chem. Rev.* **2000**, *209*, 263–331.
- (15) Avila, A.; Gregory, B. W.; Niki, K.; Cotton, T. M. *J. Phys. Chem. B* **2000**, *104*, 2759–2766.
- (16) Saccucci, T. M.; Rusling, J. F. *J. Phys. Chem. B* **2001**, *105*, 6142–6147.
- (17) Murgida, D. H.; Hildebrandt, P. *Angew. Chem., Int. Ed.* **2001**, *40*, 728–731.
- (18) Murgida, D. H.; Hildebrandt, P. *J. Phys. Chem. B* **2001**, *105*, 1578–1586.
- (19) Murgida, D. H.; Hildebrandt, P. *J. Am. Chem. Soc.* **2001**, *123*, 4062–4068.
- (20) Murgida, D. H.; Hildebrandt, P. *J. Mol. Struct.* **2001**, *565*–566, 97–100.
- (21) Chi, Q.; Zhang, J.; Anderson, J. E. T.; Ulstrup, J. *J. Phys. Chem. B* **2001**, *105*, 4669–4679.
- (22) Zhang, J.; Chi, Q.; Kuznetsov, A. M.; Hansen, A. G.; Wackerbarth, H.; Christensen, H. E. M.; Anderson, J. E. T.; Ulstrup, J. *J. Phys. Chem. B* **2002**, *106*, 1132–1152.
- (23) Jeuken, L. J. C.; McEvoy, J. P.; Armstrong, F. A. *J. Phys. Chem. B* **2002**, *106*, 2304–2313.
- (24) Hildebrandt, P.; Murgida, D. H. *Bioelectrochemistry* **2002**, *55*, 139–143.
- (25) Niki, K.; Sprinkle, J. R.; Margoliash, E. *Bioelectrochemistry* **2002**, *55*, 37–40.
- (26) Franzen, S.; Goldstein, R. F.; Boxer, S. G. *J. Phys. Chem.* **1990**, *94*, 5135–5149.
- (27) Gopher, A.; Blatt, Y.; Schönfeld, M.; Okamura, M. Y.; Feher, G. *Biophys. J.* **1985**, *48*, 311–320.
- (28) Popovic, Z. D.; Kovacs, G. J.; Vincett, P. S.; Alegria, G.; Dutton, P. L. *Chem. Phys.* **1986**, *110*, 227–237.
- (29) Wackerbarth, H.; Klar, U.; Günther, W.; Hildebrandt, P. *Appl. Spectrosc.* **1999**, *53*, 283–291.
- (30) Döpner, S.; Hildebrandt, P.; Mauk, A. G.; Lenk, H.; Stempf, W. *Spectrochim. Acta* **1996**, *A51*, 573–584.
- (31) Brautigan, D. L.; Ferguson-Miller, S.; Margoliash, E. *Methods Enzymol.* **1978**, *53D*, 128–164.
- (32) Chidsey, C. E. D. *Science* **1991**, *251*, 919–251.
- (33) Chi, Q.; Dong, S. *J. Electroanal. Chem.* **1993**, *348*, 377–388.
- (34) Marcus, R. A.; Sutin, N. *Biochim. Biophys. Acta* **1985**, *811*, 265–322.
- (35) The good agreement for  $\lambda$  obtained by different approaches confirms the assumption that the reorganization energy can be considered to be *T*-independent in the temperature range studied in this work.
- (36) Scott, R. A. Long-range intermolecular electron-transfer reactions in cytochrome *c*. In *Cytochrome c—an interdisciplinary approach*; Scott, R. A., Mauk, A. G., Eds.; University Science Books: Sausalito, CA, 1995; pp 515–541.
- (37) Cheng, J.; Terrettaz, S.; Blankman, J. I.; Miller, C. J.; Dangi, B.; Guiles, R. D. *Isr. J. Chem.* **1997**, *37*, 259–266.
- (38) Gao, Y.; McLendon, G.; Pielak, G. J.; Williams, R. J. P. *Eur. J. Biochem.* **1992**, *204*, 337–352.
- (39) Basu, G.; Kitao, A.; Kuki, A.; Go, N. *J. Phys. Chem. B* **1998**, *102*, 2085–2094.
- (40) Muegge, I.; Qi, P. X.; Wabd, A. J.; Chu, Z. T.; Warshel, A. J. *J. Phys. Chem. B* **1997**, *101*, 825–836.
- (41) The apparent redox potentials vary with the chain length, which, however, results from the potential drops across the electrode/SAM/protein interfaces and does not represent a variation of the intrinsic redox potential.<sup>18</sup>
- (42) Williams, R. J. P. *J. Solid State Chem.* **1999**, *145*, 488–495.
- (43) Neumann, E. *Prog. Biophys. Mol. Biol.* **1986**, *47*, 197–231.
- (44) Most likely the same electric field effects control the interfacial redox process of cytochrome *c*<sub>552</sub> adsorbed on a bare Ag electrode such that the low value for  $\lambda$  obtained from  $\eta$ -dependent measurements reflects the coupling of ET and PT (Lecomte, S.; Hildebrandt, P.; Soulimane, T. *J. Phys. Chem. B* **1999**, *103*, 10053–10064).
- (45) Kuznetsov, A. M.; Ulstrup, J. *Can. J. Chem.* **1999**, *77*, 1085–1096.
- (46) Krishtalik, L. I. *Biochim. Biophys. Acta* **2000**, *1458*, 6–27.
- (47) Jonsson, T.; Glickman, M. H.; Sun, S.; Klinman, J. P. *J. Am. Chem. Soc.* **1996**, *118*, 10319–10320.
- (48) Kohen, A.; Klinman, J. P. *Acc. Chem. Res.* **1998**, *31*, 397–404.
- (49) Basran, J.; Sutcliffe, M. J.; Scrutton, N. S. *Biochemistry* **1999**, *38*, 3218–3222.
- (50) Basran, J.; Patel, S.; Sutcliffe, M. J.; Scrutton, N. S. *J. Biol. Chem.* **2001**, *276*, 6234–6242.
- (51) Cha, Y.; Murray, C. J.; Klinman, J. P. *Science* **1989**, *243*, 1325–1330.
- (52) Farver, O.; Zhang, J.; Chi, Q.; Pecht, I.; Ulstrup, J. *Proc. Natl. Acad. Sci. U.S.A.* **2001**, *98*, 4426–4430.
- (53) Chen, K. S.; Hirst, J.; Camba, R.; Bonagura, C. A.; Stout, C. D.; Burgess, B. K.; Armstrong, F. A. *Nature* **2000**, *405*, 814–817.
- (54) Hirst, J.; Jameson, G. N. L.; Allen, J. J. W. A.; Armstrong, F. A. *J. Am. Chem. Soc.* **1998**, *120*, 11994–11999.
- (55) Various spectroscopic techniques including nuclear magnetic resonance, circular dichroism, UV–vis absorption, and resonance Raman spectroscopy do not provide any indications for *T*-induced conformational changes of Cyt-*c* in this temperature range (Banci, L.; Bertini, I.; Spyroulias, G. A.; Turano, P. *Eur. J. Inorg. Chem.* **1998**, 583–591. Filosa, A.; English, A. M. *J. Bioinorg. Chem.* **2000**, *5*, 448–454. Oellerich, S.; Wackerbarth, H.; Hildebrandt, P. *J. Phys. Chem. B* **2002**, *106*, 6566–6580).
- (56) The present results cannot distinguish between a one-step or a two-step mechanism.<sup>19</sup> The latter mechanism is not in contradiction with the fact that no intermediate species was observed in the TR SERR spectra because it would be populated only to a very small extent. However, such an intermediate might correspond to the species that was cryogenically trapped during the radiolytic reduction of Cyt-*c* and found to exhibit small differences in RR spectrum compared to the stable reduced form (Cartling, B. *Biophys. J.* **1983**, *43*, 191–205). This species might correspond to a reduced Cyt-*c* in which protein structure reorganization is not completed.
- (57) Rivas, L.; Murgida, D. H.; Hildebrandt, P. *J. Phys. Chem. B* **2002**, *106*, 4823–4830.
- (58) Simaan, J.; Murgida, D. H.; Hildebrandt, P. *Biopolym. (Biospectrosc.)* **2002**, *67*, 331–334.
- (59) Wackerbarth, H.; Murgida, D. H.; Oellerich, S.; Döpner, S.; Rivas, L.; Hildebrandt, P. *J. Mol. Struct.* **2001**, *563*–564, 51–59.
- (60) Michel, H.; Behr, J.; Harrenga, A.; Kannt, I. *Annu. Rev. Biophys. Biomol. Struct.* **1998**, *27*, 329–356.
- (61) Wang, K.; Zhen, Y.; Sadoski, R.; Grinnell, S.; Geren, L.; Ferguson-Miller, S.; Durham, B.; Millet, F. *J. Biol. Chem.* **1999**, *274*, 38042–38050.
- (62) Hill, B. C. *J. Biol. Chem.* **1994**, *269*, 2419–2425.
- (63) Malatesta, F.; Antonini, G.; Sarti, P.; Brunori, M. *Biophys. Chem.* **1995**, *54*, 1–33.
- (64) Nagel, G.; Kelety, B.; Möckel, B.; Büldt, G.; Bamberg, E. *Biophys. J.* **1998**, *74*, 403–412.